Experimental generation of steering odd dark beams of finite length

A. Dreischuh and D. Neshev

Department of Quantum Electronics, Sofia University, 5, J. Bourchier Boulevard, BG-1164 Sofia, Bulgaria

G. G. Paulus

Max-Planck-Institut für Quantenoptik, Hans-Kopfermann-Strasse 1, D-85748 Garching, Germany

H. Walther

Max-Planck-Institut für Quantenoptik, Hans-Kopfermann-Strasse 1, D-85748 Garching, Germany, and Sektion Physik, Ludwig-Maximillians-Universität, Am Coulombwall 1, D-85747 Garching, Germany

Received March 2, 2000; revised manuscript received August 15, 2000

We report what we believe is the first realization of odd dark beams of finite length under controllable initial conditions. We obtain mixed edge–screw phase dislocations by reproducing binary computer-generated holograms. Two effective ways to control the steering of the beams are analyzed experimentally and compared with numerical simulations. © 2000 Optical Society of America [S0740-3224(00)01412-0]

OCIS codes: 190.4420, 190.5940, 090.1760.

1. INTRODUCTION

Physically, dark spatial solitons (DSS's) are localized intensity dips that appear in stable background beams as the result of an exact counterbalance of diffraction and nonlinearity. A necessary condition for their existence is the presence of a phase dislocation in the wave front along which the phase is indeterminate and the field amplitude is zero. Besides by their intriguing physical picture, particular interest in DSS's is motivated by their ability to induce gradient optical waveguides in bulk self-defocusing nonlinear media.[1–5] The only known truly two-dimensional DSS's are the optical vortex solitons (OVS's),[2] whereas in one transverse spatial dimension DSS's manifest themselves as dark stripes.[6] The odd initial condition required for generating a fundamental one-dimensional (1D) DSS corresponds to an abrupt π-phase jump centered along the irradiance minimum of the stripe. The OVS's have a more complicated phase profile described by $\exp(im\varphi)$, where φ is the azimuthal coordinate in a plane perpendicular to the background beam propagation direction and m—the so-called topological charge—is an integer number. This phase function ensures a π phase jump in each diametrical slice through the vortex core. Fundamental DSS's of these types have the common feature of zero transverse velocity if no perturbations are present. In contrast, ring dark solitary waves[7] slowly change their parameters, even when they originate from ideal odd initial conditions.[8]

In their pioneering research, Nye and Berry[9] conjectured that mixed edge–screw dislocations cannot exist. Nonetheless, almost two decades later an indication of their existence was found[10] for two interacting optical vortices of opposite topological charges. In our recent experiments on the generation of quasi-two-dimensional DSS's,[11] we found that moderate saturation of the nonlinearity can stabilize the snake instability that usually leads to the solitons' decay. This made it possible to identify 1D odd dark beams (ODB's) of finite length with their characteristic edge–screw phase dislocations.[11,12] The mixed dislocation forces the dark beams to steer in space. This property appears to be of practical interest,[12] provided that there are effective ways to control the ODB's transverse velocity.

In this paper we report what is to our knowledge the first experimental realization of steering of ODB's of finite length with mixed phase dislocations under controllable initial conditions. Two approaches to controlling the beams' transverse velocity are investigated experimentally and compared with numerical simulations.

2. EXPERIMENTAL SETUP AND RESULTS

A. Computer-Generated Holograms

The phase portrait of the mixed edge–screw dislocation[12] consists of a pair of semihelices with a phase difference of π to which an effective topological charge of $\pm 1/2$ can be ascribed [Fig. 1(a)]. Their spatial offset $2b$ determines the length of the edge part of the dislocation and ensures a phase jump of $\Delta\varphi$ in the direction perpendicular to the dark stripe of finite length. The phase function of this mixed phase dislocation can be described by

$$\Phi_{\alpha,\beta}(x,y) = \Delta\varphi\left[-\frac{\beta}{\pi}\arctan\left(\frac{\alpha x}{y + b\beta}\right) + \frac{(1-\alpha)}{2}\operatorname{sgn}(x)\right], \tag{2.1}$$

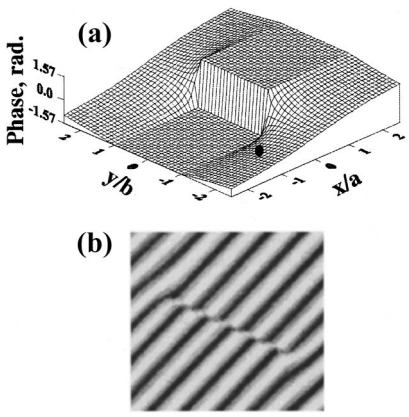

Fig. 1. (a) Phase distribution and (b), interference pattern corresponding to a mixed edge–screw phase dislocation.

where x and y denote the transverse Cartesian coordinates perpendicular and parallel, respectively, to the dark beam. $2b$ stands for the length of the edge part of the dislocation, and

$$\alpha = \begin{cases} 0 & |y| \leq b \\ 1,\ \beta = -1 & y > b \\ 1,\ \beta = 1 & y \leq -b \end{cases}. \qquad (2.2)$$

The pattern of computer-generated holograms (CGH's) that we used to produce this phase distribution comprises parallel lines that become curved at the positions of the semivortex cores [Fig. 1(b)]. In the edge part of the dislocation the lines terminate and reappear shifted for a π jump by one half of the pattern period. Holograms with such structures correspond to interference lines shifted along an imaginary line of finite length and to curved lines that limit the dislocations, as was recently observed experimentally.[11] The binary CGH's used are photolithographically fabricated, with a grating period of 20 μm. Several holograms with various lengths of the edge parts of the dislocations are etched upon a common substrate. Special attention was paid to aligning the edge parts of the various dislocations correctly upon their common substrate. The simplicity of varying the dislocation length and the magnitude of the phase jump is the main advantage[13] of the approach that we have chosen. The diffraction efficiency at first order is 9%, close to the theoretical 10% limit for binary holograms. The unavoidable quantization inaccuracy of $\pi/24$ (Ref. 14) for holograms of this type is negligible for the measurements with phase jumps of $\Delta\varphi = 3\pi/4, \pi, 5\pi/4$ that are presented here.

B. Experimental Setup

The setup used is similar to that which was used for the research presented in the previous experiment.[11] Briefly, we use the beam of a single-line Ar^+ laser ($\lambda = 488$ nm) to reconstruct the CGH's. The first-diffraction-order beam with the phase dislocation nested in it is filtered through a slit and is focused onto the entrance of a 10-cm-long nonlinear medium (NLM). After the desired propagation path length, the beam is deflected by a prism immersed in a nonlinear liquid and is projected directly onto a CCD camera array with a resolution of 13 μm. The NLM is ethylene glycol dyed with diethyloxadicarbocyanine iodine (Lambdachrome) to reach an absorption coefficient of 0.107 cm^{-1}. In a calibration measurement we generated 1D DSS's by using CGH's of the type described in Subsection 2.A. The soliton constant Ia^2 (i.e., the product of the background beam's intensity I and the square of the dark beam width a measured at the $1/e$ level) was found to reach its asymptotically constant value for input powers of $P_{\mathrm{sol}}^{1D} \approx 33$ mW. It is known that thermally self-defocusing liquids are both nonlocal and saturable. Inasmuch as the saturation of the nonlinearity is able to modify the ODB's transverse velocity and profile, we needed to estimate that saturation and to account for it in our numerical calculations. In an independent measurement we realized a self-bending scheme similar to that used in the research reported in Refs. 15 and 16. The asymmetry required was introduced by an intentional tilt of the prism immersed in the NLM, which yielded different nonlinear propagation path lengths for the different parts of the background beam. The strength of the self-bending effect was measured in the near field. For an absorptive nonlocal medium the choice of a suitable saturation model is not trivial;[17] see also Sec. IV of Ref. 18. We found a good fit for the experimental data to the expression $\Delta y \sim I/(1 + I/I_{\mathrm{sat}})^{\gamma}$. Using it, we estimated $P_{\mathrm{sat}} \approx 100$ mW and $\gamma = 3$. In addition to carefully aligning the CGH's upon the substrate, we reproduced the holograms such as to achieve vertical dark beam steering, which is not sensitive to the possible presence of undesired weak horizontal self-deflection of the background beam. We changed the ODB parameters (length-to-width ratio and magnitude of the phase jump) by a strict horizontal translation of the substrate. We tested the accuracy of the alignment by checking for equal steering of the ODB's reproduced from two identical holograms placed at opposite ends of the series of aligned CGH's. Here we identify the ODB's by the corresponding lengths $2b$ of the edge portions of the dislocations in CGH pixels (1 pixel = 5 μm) as encoded in the holograms. The deflection Δx of the dark beams is measured in units of CCD camera pixels. We estimate that measurements with an encoded dislocation length of $b/5\ \mu$m CGH pixels correspond to a dislocation length–to–ODB width ratio $(2b/a) = 2 \times 0.1 \times (b/5\ \mu\mathrm{m})$ in the numerical simulations (e.g., a 14-pixel, dislocation length corresponds to $b/a = 1.4$ in the simulations).

C. Odd Dark Beam Steering Versus Dislocation Length

All data presented in this subsection refer to π phase jumps across the edge parts of the mixed dislocations. In Fig. 2(a) we plot the deflection Δx of ODB's with several dislocation lengths for input powers of 1.7 mW (filled circles), 33 mW (filled triangles), and 67 mW (open squares). The data obtained at $P = 1.7$ mW refer to a linear regime of propagation. Some experimental frames obtained at 33 and 67 mW are shown in Figs. 2(b) and 2(c), respectively. They were recorded for a nonlinear propagation path length of $z = 8.5$ cm. The general tendency of a linear increase of the deflection with decreasing dislocation length is clearly expressed [Fig. 2(a), solid curve]. The shortest mixed phase dislocation encoded

was only 1 pixel long. In this case the strong deviation from the linear dependence is caused by the annihilation of the semicharges that is due to the shortening of the edge part of the dislocation. It is shown below that this shortening accelerates at higher input powers (intensities). For that reason, even the ODB with an initially 10 pixel long phase dislocation appears gradually less deflected at $P = 67$ mW than for $P = 33$ mW [Fig. 2(a)]. In Figs. 2(b) and 2(c) the upper solid lines are intended to denote the positions of the ODB's at the entrance of the NLM. Because ODB steering is also present in the linear regime of propagation [Fig. 2(a), filled circles] these positions (with respect to the dark beam's intensity minimum and the trailing peak maximum) are identified by numerical simulations for $b/a = 2.5$. The identification corresponds to an encoded dislocation length of 25 pixels [not shown in Figs. 2(b) and 2(c)]. Somewhat surprising is the weak sensitivity of the ODB deflection-versus-background beam power (intensity) far from topological charge annihilation, which we can intuitively understand by recalling the known interaction situation of well-separated OVS's of opposite topological charges.[19,20] In this case the attraction between the OVS's is negligible as compared with their translation as a pair. We measured the ODB deflection versus nonlinear propagation path length at a constant input power of 33 mW (see Fig. 3). As expected, the ODB with a 10-pixel-long dislocation has higher transverse velocity than the ODB with a 22-pixel-long dislocation. The linearity in the dependencies is also well pronounced.

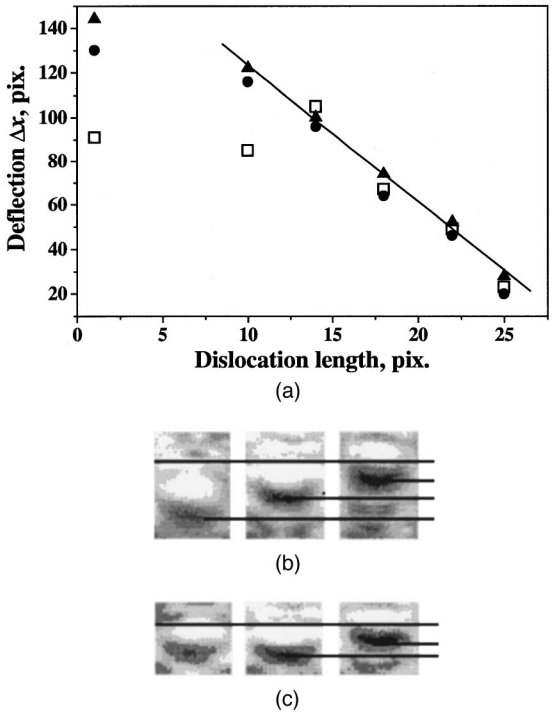

Fig. 2. (a) Deflection of odd dark beams of finite length versus dislocation length at input powers of 1.7 mW (filled circles), 33 mW (filled triangles), and 67 mW (open squares) for $z = 8.5$ cm and $\Delta\varphi = \pi$. Selected experimental frames are shown in (b), 33 mW and (c), 67 mW. From left to right, the frames correspond to $b = 1, 14, 22$ pixels. Upper solid lines, calculated position of the ODB at the entrance of the NLM for $b = 25$ pixels.

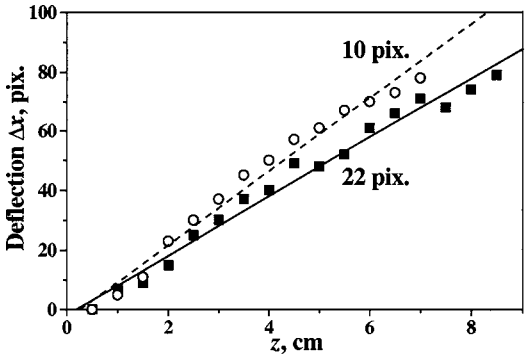

Fig. 3. Deflection Δx versus nonlinear propagation path length z for encoded dislocation lengths of 10 and 22 pixels. Dashed and solid curves, the respective linear fits. $P = 33$ mW, $\Delta\varphi = \pi$.

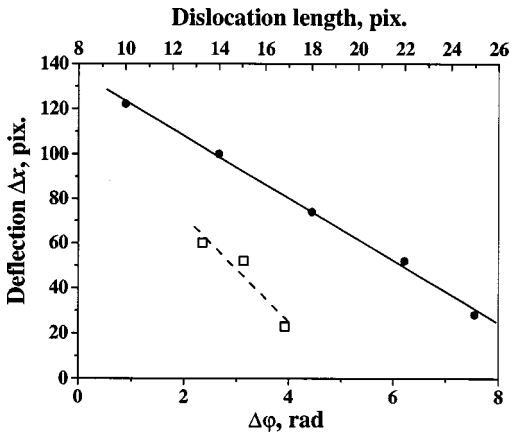

Fig. 4. ODB deflection versus magnitude of phase jump $\Delta\varphi$ (open squares) and dislocation length as encoded in the CGH's (filled circles). Solid curves are linear fits. $P = 33$ mW.

D. Phase Control of the Odd Dark Beam Steering

As a second possible way to control the dark-beam deflection we considered varying the magnitude of the phase jump $\Delta\varphi$ across the edge part of the mixed dislocation. In Fig. 4 we compare the experimental dependencies $\Delta x(\Delta\varphi)|_{b=22\text{pix}}$ (open squares) and $\Delta x(b)|_{\Delta\varphi=\pi}$ (filled circles). The lines are the respective linear fits. Because a problem in encoding a larger set of phase jumps in the CGH's was recognized too late, we measured the deflection Δx at $\Delta\varphi = 3\pi/4, \pi, 5\pi/4$ only. In view of the limited points of measurement, the linear fit of the phase dependence in Fig. 4 appears to be assailable. The linearity of the dependence, however, is confirmed by numerical simulations (see Section 3 below). We have plotted the dependence of Δx on $\Delta x(\Delta\varphi)$ and on $\Delta x(b)$ in one figure to underline the fact that it appears to be easier to deflect the ODB by controlling the phase than by controlling the dislocation length. The measurements are performed at a constant power of 33 mW.

E. Power/Intensity Dependencies

The ability of dark spatial solitons[1–5] (and dark spatial waves[21,22]) to induce gradient all-optical waveguides in bulk self-defocusing NLM's originates in the negative nonlinear correction to the linear refractive indices of the media. Therefore, the intensity dependencies remain un-

questionably of interest, despite the low sensitivity of the ODB steering to the input power (intensity). In Fig. 5 we present experimental data on the power dependence of the length of the edge portion of the mixed dislocation for $\Delta\varphi = \pi$ and for two different lengths (14 and 22 pixels) encoded in the holograms. It is easy to understand that the (mixed) phase dislocations do not remain sharp and at an unchanged magnitude when the (odd) dark beam is steering.[23] We estimate the dislocation lengths by evaluating the respective longitudinal ODB slices at 5% of the background-beam intensity (i.e., at the actual noise level in the recorded frames). Generally, the dislocation length decreases monotonically with increasing input power. Asymptotically, the dislocation flattens and disappears, provided that the ratio b/a is less than 2. As was mentioned in Ref. 12, at $b/a \sim 4$ the ODB's should be expected to bend owing to snake instability.[17] In fact, we observed such behavior for ODB's with encoded dislocation lengths that ranged from 4 to 6. Creation of a vortex beam is recognized by the convergence of two neighboring interference lines into one. However, the vortices formed by this instability remain with highly overlapping cores.[17,24]

In Fig. 6 we plot the measured ODB widths (Fig. 6a) and lengths (Fig. 6b) at the 1/*e* level as a function of the background-beam power. The initial lengths of the mixed phase dislocations are denoted in pixels as encoded on the respective CGH's, whereas the widths and lengths at the exit of the NLM are measured in units of CCD camera pixels. The strong decrease in both the ODB width and length up to 17 mW (approximately $P_{\mathrm{sol}}^{1\mathrm{D}}/2$) is followed by recovery of the width and length at approximately $P_{\mathrm{sol}}^{1\mathrm{D}}$. At higher input powers, both transverse quantities decrease, but the tendency is slower than for the situation below $P_{\mathrm{sol}}^{1\mathrm{D}}/2$ and stabilizes asymptotically at high saturation. As is discussed in Section 3, the minima in the curves plotted in Fig. 6 result from the reshaping of the ODB's at the particular 1/*e* intensity level chosen for evaluation. The estimation there shows that the first rapid decrease in both transverse dimensions of the ODB's does not correspond to a soliton constant formation. Generally speaking, the ODB's analyzed are not solitary waves in the widely adopted sense, inasmuch as they do not survive, for instance, a collision with a second ODB that is steering in the opposite direction.[12] Nevertheless, the narrowing in both transverse directions for higher powers (intensities) should improve the guiding ability when signal beams or pulses are to be transmitted inside the ODB's and deflected in space.[25] It is interesting to note that, independently of the length of the mixed dislocations ($2b$), the widths (a) of the dislocations should be initially equal (in the near field behind the CGH's), but appear to be different near the entrance of the NLM. The estimation has shown a CGH-to-NLM distance of approximately four Rayleigh diffraction lengths with respect to the initial ODB width. The well-pronounced separation between the curves in Fig. 6a should be attributed to the different two-dimensional diffractions at different initial ODB length-to-width ratios.

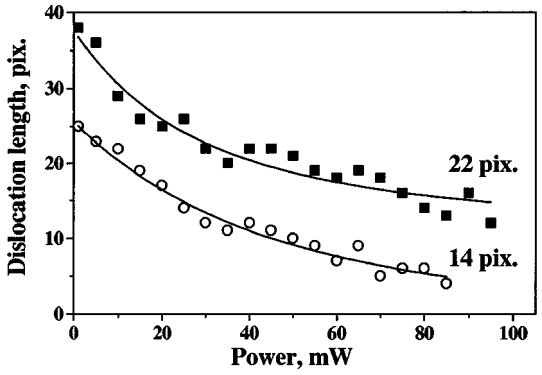

Fig. 5. Edge dislocation length versus input background beam power for two dislocation lengths encoded in the CGH's. $\Delta\varphi = \pi$, $z = 8.5$ cm.

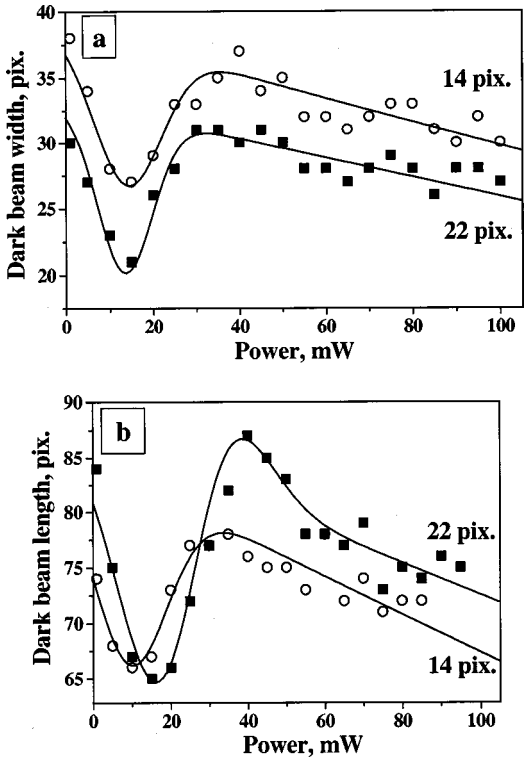

Fig. 6. ODB a, width and b, length (at the 1/*e* level) versus input background-beam power for two different dislocation lengths encoded in the CGH's. $z = 8.5$ cm.

3. NUMERICAL SIMULATIONS

In our numerical simulations we are modeling the experimentally obtained dependencies by accounting for the estimated moderate saturation of the nonlinearity. The saturation was described by the phenomenologically adopted correction to the nonlinear refractive index:

$$\Delta n = n_2|E|^2/(1 + s|E|^2)^{\gamma} \tag{3.1}$$

(see Ref. 1 for details). Within this model [Eq. (3.1)] the saturable nonlinearity tends to Kerr nonlinearity for low intensities. We determined the three independent parameters [I_{sat}, γ, and $(|n_2|I_0)_{\mathrm{max}}$] in Eq. (3.1) by evaluating the data from the self-bending experiment described in Subsection 2.B. The estimated values $P_{\mathrm{sol}}^{1\mathrm{D}} = 33$ mW, $P_{\mathrm{sat}} = 100$ mW, $\gamma = 3$, and $\Delta n = (|n_2|I_0)_{\mathrm{max}} = 10^{-3}$ are accurate to within 15%.

The (2 + 1)-dimensional nonlinear evolution of the steering ODB of finite length in the bulk homogeneous and isotropic NLM is described by the generalized nonlinear Schrödinger equation

$$i\frac{\partial E}{\partial \zeta} + \frac{1}{2}\left(\frac{\partial^2}{\partial \xi^2} + \frac{\partial^2}{\partial \eta^2}\right)E - \frac{L_{\mathrm{Diff}}}{L_{\mathrm{NL}}}\frac{|E|^2}{(1 + s|E|^2)^{\gamma}}E = 0, \tag{3.2}$$

where the transverse spatial coordinates are normalized to the initial dark-beam width ($\zeta = x/a$, $\eta = y/a$) and the propagation path length is expressed in Rayleigh diffraction lengths $L_{\mathrm{Diff}} = ka^2$. Further, $L_{\mathrm{NL}} = (kn_2I_0)^{-1}$ is the nonlinear length, k is the wave number inside the NLM, and I_0 is the background beam's intensity. $s = P_{\mathrm{sol}}^{1\mathrm{D}}/P_{\mathrm{sat}} = 0.3$ is the saturation parameter. As was done in the research reported in Ref. 12, the slowly varying electric-field amplitude of the ODB was chosen to be tanh shaped:

$$E(x,y) = \sqrt{I_0}B[r_{1,0}(x,y)]\tanh\left[\frac{r_{\alpha,\beta}(x,y)}{a}\right] \times \exp[i\Phi_{\alpha,\beta}(x,y)], \tag{3.3}$$

where $r_{\alpha,\beta}(x,y) = [x^2 + \alpha(y + \beta b)^2]^{1/2}$ is the effective Cartesian–radial coordinate, $\Phi_{\alpha,\beta}$ is the phase distribution of the mixed edge–screw dislocation [see Eq. (2.1)], and α and β are given by Eq. (2.2). The width w of the super-Gaussian background beam

$$B(r) = \exp\left\{-\left[\left(\frac{x^2 + y^2}{w^2}\right)^{1/2}\right]^{14}\right\} \tag{3.4}$$

is chosen to exceed at least 15 times the ODB lengths. Model equation (3.2) was solved numerically by the beam-propagation method on a 1024 × 1024 grid. It should be mentioned that the initial width $a(z = 0)$ of the ODB of finite length was chosen to correspond to that of an infinite 1D dark spatial soliton ($a = a_{\mathrm{sol}}^{1\mathrm{D}} = \mathrm{const}\, I_0^{-1/2}$). It was proved numerically that the ODB deflection is insensitive to the particular value of a, and Figs. 7–9 were generated under this assumption. In fact, the nonlinearity causes appreciable reshaping of the beams, in particular in the first evolution stage when the ODB starts steering; see Fig. 2 of Ref. 12.

To improve the similarity between the experimental data (Figs. 5 and 6) and the numerical results (Fig. 10), we assume an initial ODB width that is twice as large as in the experiment. In Fig. 7 we plot the ODB deflection versus $b/a|_{z=0}$ for several input powers (intensities). All data presented in this section refer to a normalized propagation path length of $z = 4L_{\mathrm{NL}}$, which corresponds to that estimated for the experiment. Nevertheless, all calculations are carried out up to $10L_{\mathrm{NL}}$, whereby no qualitative deviation from the tendencies discussed is seen. The linearity in the ODB deflection versus b/a is well obeyed except for $b/a > 2.2$. The longer ODB's steer more slowly, bend slightly, and decay into pairs of vortex beams for $b/a > 4$. In the linear regime of propagation the ODB's also are deflected but the deflection is stronger at higher input powers/intensities. This tendency is more pronounced for shorter dislocations. In the experimental data (Fig. 2a), this behavior is much weaker, and the deflection remains within the experimental accuracy. Looking for an adequate explanation, in a series of simulations we verified that a ±30% inaccuracy in estimating P_{sat} results in only a ±5% deviation in the ODB deflection at $z = 4L_{\mathrm{NL}}$. The observed tendency of a decrease of the ODB steering velocities at increased saturation is well understood[26] but seems to be insufficient in quantity. We attribute the absence of a well-expressed power dependence in Fig. 2a to the NLM nonlocality. In a separate experiment it was estimated that the nonlocality in this

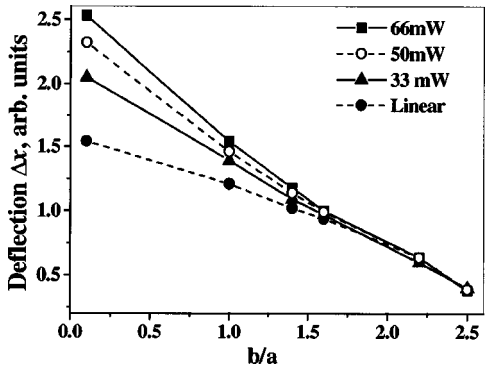

Fig. 7. Calculated ODB steering versus b/a for several input powers ($\Delta\varphi = \pi$).

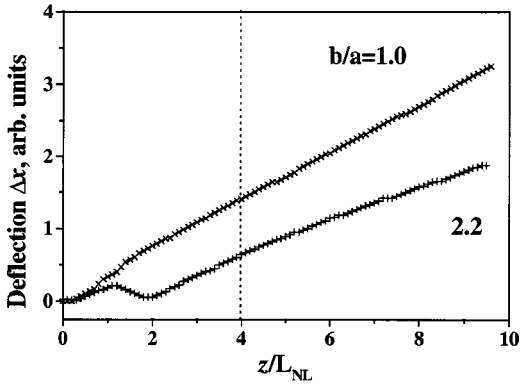

Fig. 8. ODB steering along the NLM for $b/a = 1.0$, 2.2. Crosses, 10% of the numerical data. Vertical dashed line, propagation distance $z/L_{\mathrm{NL}} = 4$, corresponding to the experimental conditions at 33 mW.

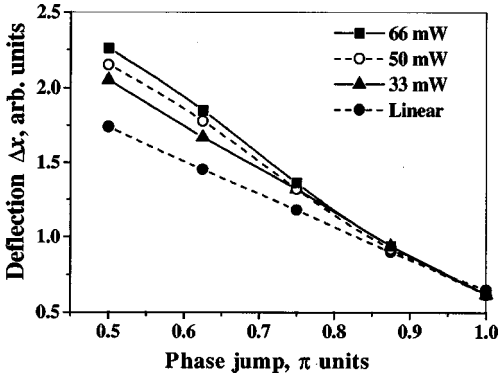

Fig. 9. Deflection of ODB's versus phase jump $\Delta\varphi$ for $b/a = 2.2$ and for several input powers.

medium is negligible on a spatial scale of several hundred of micrometers only.[18]

In Fig. 8 we plot the ODB deflection versus the nonlinear propagation path length z/L_{NL} for $b/a = 1.0, 2.2$. As in Fig. 7, the magnitude of the edge part of the phase dislocation is set to $\Delta\varphi = \pi$. Once the ODB starts to steer, its transverse velocity remains constant (see Fig. 3). The longer ODB's with longer edge dislocations, however, emit dispersive waves in their first evolution stage ($z < 1L_{\mathrm{NL}}$), which cause a delay in the steering along the NLM (Fig. 8, lower curve).

In Fig. 9 we present results obtained for phase-dependent control of the ODB deflection at several input powers (intensities). In qualitative agreement with the experimental observation, the linear increase in ODB steering with a decrease in the magnitude of the phase jump to $\Delta\varphi = 0.5\pi$ is evident. A comparison of Figs. 7 and 9 confirms the conclusion that at a fixed nonlinear propagation distance the phase-controlled ODB deflection is more efficient than that which one can achieve by varying the b/a ratio.

Figure 10a is intended to clarify the origin of the nonmonotonic power dependencies of the ODB widths (and lengths) observed at input powers below $P_{\mathrm{sol}}^{1\mathrm{D}}$ (see Fig. 6). The solid curve represents the ODB FWHM; the dashed curve, the full width at the $1/e$-intensity level. In these simulations $\Delta\varphi = \pi$ and $b/a = 1.4$ are assumed. Qualitatively, we obtained the same curves for $b/a = 2.2$ by accounting for the initial free-space propagation in the experiment (from the CGH to the entrance of the NLM; $z \approx 4L_{\mathrm{Diff}}$). The minimum in the ODB width evaluated at the $1/e$ level originates from the reshaping of the beam profile that is caused by the moderate saturation. A similar reshaping is reported in Ref. 27 (see Figs. 2–4 therein). At $b/a = 2.2$ the data obtained for the ODB length versus input power (intensity) were found to be even more sensitive to the intensity level of evaluation. Because of the transverse steering of the ODB's of finite length, the edge portions of the dislocations shorten monotonically with increasing background power (Fig. 10b). The numerical results are in very good qualitative agreement with the experimental ones (Fig. 5).

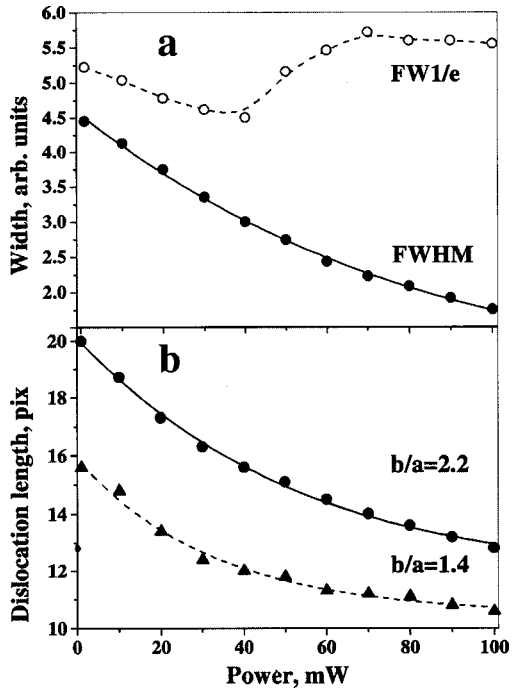

Fig. 10. a, ODB width and b, length of the edge portion of the mixed phase dislocation versus input power for $\Delta\varphi|_{z=0} = \pi$ and $b/a = 1.4$. (FW1/e, full width at the $1/e$-intensity level.)

4. CONCLUSION

The results presented show that one can effectively control the inherent steering dynamics of odd dark beams of finite length by varying both the magnitude $\Delta\varphi$ and the relative length b/a of the mixed edge–screw phase dislocation. The background-beam intensity has a weak influence on the steering but is important for keeping the optically induced gradient waveguides steep, which is crucial for all-optical guiding, deflection, and switching of signal beams or pulses. Because the mixed phase dislocations shorten and flatten along the nonlinear media (tending asymptotically to washout), the ODB's seem to be promising for use primarily in future short-range all-optical switching devices.

ACKNOWLEDGMENTS

A. Dreischuh thanks the Alexander von Humboldt Foundation for the award of a fellowship and for the opportunity to work in the stimulating atmosphere of the Max-Planck-Institut für Quantenoptik (Garching, Germany). This study was also supported by the National Science Foundation of Bulgaria.

A. Dreischuh's e-mail address is ald@phys.uni-sofia.bg, G. G. Paulus's e-mail address is ggp@mpq.mpg.de, and that of H. Walther is prof.h.walther@mpq.mpg.de.

REFERENCES

1. Yu. S. Kivshar and B. Luther-Davies, "Dark optical solitons: physics and applications," Phys. Rep. **298**, 81–197 (1998).
2. G. Swartzlander, Jr., and C. Law, "Optical vortex solitons observed in Kerr nonlinear medium," Phys. Rev. Lett. **69**, 2503–2506 (1992).
3. E. A. Ostrovskaya and Yu. S. Kivshar, "Nonlinear theory of soliton-induced waveguides," Opt. Lett. **23**, 1268–1270 (1998).
4. A. H. Carlsson, J. N. Malmberg, E. A. Ostrovskaya, T. J. Alexander, D. Anderson, M. Lisak, and Yu. Kivshar, "Linear and nonlinear waveguides induced by optical vortex solitons," Opt. Lett. **25**, 660–662 (2000).
5. C. T. Law, X. Zhang, and G. A. Swartzlander, Jr., "Waveguiding properties of optical vortex solitons," Opt. Lett. **25**, 55–57 (2000).
6. G. Allan, S. Skinner, D. Andersen, and A. Smirl, "Observation of fundamental dark spatial solitons in semiconductors using picosecond pulses," Opt. Lett. **16**, 156–158 (1991).
7. Yu. S. Kivshar and X. Yang, "Ring dark solitons," Phys. Rev. E **50**, R40–R43 (1994); "Dynamics of dark solitons," Chaos, Solitons Fractals **4**, 1745–1758 (1994).
8. D. Neshev, A. Dreischuh, V. Kamenov, I. Stefanov, S. Dinev, W. Fliesser, and L. Windholz, "Generation and intrinsic dynamics of ring dark solitary waves," Appl. Phys. B **64**, 429–433 (1997).

9. J. F. Nye and M. V. Berry, "Dislocations in wave trains," Proc. R. Soc. London, Ser. A **336**, 165–190 (1974).
10. V. Bazhenov, M. Soskin, and M. Vasnetsov, "Screw dislocations in light wavefronts," J. Mod. Opt. **39**, 985–990 (1992); I. Basistiy, V. Bazhenov, M. Soskin, and M. Vasnetsov, "Optics of light beams with screw dislocations," Opt. Commun. **103**, 422–428 (1993).
11. A. Dreischuh, G. G. Paulus, and F. Zacher, "Quasi-2D dark spatial solitons and generation of mixed phase dislocations," Appl. Phys. B **69**, 107–111 (1999).
12. A. Dreischuh, G. G. Paulus, F. Zacher, and I. Velchev, "Steering one-dimensional odd dark beams of finite length," Appl. Phys. B **69**, 113–117 (1999).
13. N. R. Heckenberg, R. McDuff, C. P. Smith, and A. G. White, "Generation of optical phase singularities by computer-generated holograms," Opt. Lett. **17**, 221–223 (1992).
14. W.-H. Lee, "Computer-generated holograms: techniques and applications," in *Progress in Optics*, E. Wolf, ed. (North-Holland, Amsterdam, 1978), Vol. XVI, pp. 119–229.
15. A. E. Kaplan, "Bending of trajectories of asymmetrical light beams in nonlinear media," JETP Lett. **9**, 33–36 (1969).
16. M. S. Brodin and A. M. Kamuz, "Observation of self-bending of a non-uniform intense laser beam in an NaCl crystal," JETP Lett. **9**, 351–353 (1969).
17. V. Tikhonenko, J. Christou, B. Luther-Davies, and Yu. S. Kivshar, "Observation of vortex solitons created by the instability of dark soliton stripes," Opt. Lett. **21**, 1129–1131 (1996).
18. A. Dreischuh, G. G. Paulus, F. Zacher, F. Grasbon, and H. Walther, "Generation of multiple-charged optical vortex solitons in a saturable nonlinear medium," Phys. Rev. E **60**, 6111–6117 (1999).
19. K. Staliunas, "Vortices and dark solitons in two-dimensional nonlinear Schrödinger equation," Chaos, Solitons Fractals **4**, 1783–1796 (1994).
20. D. Neshev, A. Dreischuh, M. Assa, and S. Dinev, "Motion control of ensembles of ordered optical vortices generated on finite-extent background," Opt. Commun. **151**, 413–421 (1998).
21. A. Dreischuh, V. Kamenov, and S. Dinev, "Parallel guiding of signal beams by a ring dark soliton," Appl. Phys. B **63**, 145–150 (1996).
22. D. Neshev, A. Dreischuh, S. Dinev, and L. Windholz, "Controllable branching of optical beams by quasi-2D dark spatial solitons," J. Opt. Soc. Am. B **14**, 2869–2876 (1997).
23. R. Thurston and A. Weiner, "Collisions of dark solitons in optical fibers," J. Opt. Soc. Am. B **8**, 471–477 (1991).
24. A. V. Mamaev, M. Saffman, and A. A. Zozulya, "Propagation of dark stripe beams in nonlinear media: snake instability and creation of optical vortices," Phys. Rev. Lett. **76**, 2262–2265 (1996).
25. D. Neshev, A. Dreischuh, G. G. Paulus, and H. Walther, "Directional coupling of optical signals by odd dark beams with mixed phase dislocations," http://xxx.lanl.gov/abs/nlin.PS/0007026 (2000).
26. W. Krolikowski, N. Akhmediev, and B. Luther-Davies, "Darker-than-black solitons: dark solitons with total phase shift greater than π," Phys. Rev. E **48**, 3980–3987 (1993).
27. V. Tikhonenko, Yu. S. Kivshar, V. Steblina, and A. Zozulya, "Vortex solitons in a saturable optical medium," J. Opt. Soc. Am. B **15**, 79–86 (1998).